Characterization of Hybrid CNT Polymer Matrix Composites*

Brian W. Grimsley[1], Roberto J. Cano[1], Megan C. Kinney[1], James Pressley[1], Godfrey Sauti[2], Michael W. Czabaj[1], Jae-Woo Kim[2], and Emilie J. Siochi[1]

[1] NASA Langley Research Center, Hampton, VA 23681
[2] National Institute of Aerospace, Hampton, VA 23666

ABSTRACT

Carbon nanotubes (CNTs) have been studied extensively since their discovery and demonstrated at the nanoscale superior mechanical, electrical and thermal properties in comparison to micro and macro scale properties of conventional engineering materials. This combination of properties suggests their potential to enhance multi-functionality of composites in regions of primary structures on aerospace vehicles where lightweight materials with improved thermal and electrical conductivity are desirable. In this study, hybrid multifunctional polymer matrix composites were fabricated by interleaving layers of CNT sheets into Hexcel® IM7/8552 prepreg, a well-characterized toughened epoxy carbon fiber reinforced polymer (CFRP) composite. The resin content of these interleaved CNT sheets, as well as ply stacking location were varied to determine the effects on the electrical, thermal, and mechanical performance of the composites. The direct-current electrical conductivity of the hybrid CNT composites was characterized by in-line and Montgomery four-probe methods. For $[0]_{20}$ laminates containing a single layer of CNT sheet between each ply of IM7/8552, in-plane electrical conductivity of the hybrid laminate increased significantly, while in-plane thermal conductivity increased only slightly in comparison to the control IM7/8552 laminates. Photo-microscopy and short beam shear (SBS) strength tests were used to characterize the consolidation quality of the fabricated laminates. Hybrid panels fabricated without any pretreatment of the CNT sheets resulted in a SBS strength reduction of 70%. Aligning the tubes and pre-infusing the CNT sheets with resin significantly improved the SBS strength of the hybrid composite To determine the cause of this performance reduction, Mode I and Mode II fracture toughness of the CNT sheet to CFRP interface was characterized by double cantilever beam (DCB) and end notch flexure (ENF) testing, respectively. Results are compared to the control IM7/8552 laminate.

Corresponding Author: Brian W. Grimsley, brian.grimsley@nasa.gov, (757) 864-6282

1.0 INTRODUCTION

Carbon fiber reinforced polymer (CFRP) composites are increasingly utilized as primary structure on military and commercial aircraft. The recently certified Boeing 787 Dreamliner as well as the Airbus A350 XWB are comprised of approximately 50% CFRP. In addition to the increased fuel efficiency realized from the use of CFRP structure, maintenance costs of these new jetliners are projected to be significantly lower than the previous class of aluminum aircraft. The ~20% reduction in structural weight realized from replacing aluminum with comparably

higher strength- and stiffness-to-weight toughened epoxy CFRP in the highly, tension-loaded regions of the fuselage and wing structures also results in up to 30% reduction in life-cycle maintenance costs associated with fatigue of aluminum flight structures [1]. However, incorporation of lightweight CFRP in primary structure of aircraft introduces risks. For example, it is well established that composite structures are more susceptible to lightning strike damage than metallic structures [2]. The low electrical conductivity of epoxy CFRP compared to aluminum alloy requires the application of a conductive layer of copper mesh over the CFRP structure to disperse up to 200 kA of current that can be delivered during a lightning-strike. Technologies have been developed to bond copper mesh on the surface of the CFRP laminate and adequately disperse lightning current without adding significantly structural weight [2]. At a density of 8.9g/cc for copper, the state-of-the-art (SOA) for lightning strike mitigation can benefit from the development of a multifunctional CFRP laminate with improved electrical and thermal conductivity to dissipate the energy during lightning strike with reduced weight penalty.

The potential of carbon nanotubes, was first published in 1991 by Iijima [3]. Since then, both the theoretical and measured superior nanoscale mechanical, thermal and electrical properties of CNTs have been reported [4-18]. The covalent sp^2 bonds formed between the carbon atoms in CNTs are predicted to yield an extremely high moduli of elasticity of 1.26 TPa for a tube wall thickness of 0.34 nm [4]. The first measurement of the elastic modulus of rope containing 11 multi-wall nanotubes (MWNTs) resulted in an average of 1.8 ± 0.9 TPa [5]. The elastic strain of ropes containing 10 to 100 single-wall nanotubes (SWNTs) was measured using a probe in atomic force microscopy resulting in a maximum measured strain of 5.8 ± 0.9%. The calculated failure strength of these nano-ropes is 45 ± 7 GPa [6]. For comparison, IM7 carbon fiber with an average diameter of 0.0052 mm has a reported ultimate tensile strength of 5.5 GPa and an elastic modulus of 276 GPa [7]. Zhou reports the measured resistance of a SWNT at room temperature to be 17.5 kΩ [8] which corresponds to an electrical conductivity of 4.5 $x10^5$ S/cm. For SWNTs, the axial (along the tube) thermal conductivity, k_1, has been measured at room temperature in vacuum and reported to be ≈3500 W/m•K and in the radial direction, k_3 is 1.52 W/m•K [9]. Smalley, et.al, report the electrical conductivity of 67 S/cm for an un-oriented mat containing 70% by volume SWNTs. [10]. In comparison for Hextow® IM7 carbon fiber, Hexcel reports the electrical conductivity as σ = 667 S/cm, and the thermal conductivity as k_1 = 5.40 W/m*K, [7]. The measured mechanical and physical properties of the individual CNTs are superior to these same properties reported for IM7 carbon fiber commonly used in structural aerospace composites, suggesting that retaining only a portion of the nanoscale properties of CNTs in a macroscale composite could offer a significant improvement. However, CFRP used in structural components was far more developed in comparison to the SOA of CNT-epoxy composites. The majority of the published studies for CNT composites utilize low volume (≤5 wt.%) dispersions of CNTs in polymer suspensions that yield improvements on the order of a 35% increase in tensile strength, 63% increase in Young's modulus and a significant increase in electrical conductivity relative to the matrix resin. For example, the electrical conductivity of the pristine polyethylene terephthalate (PET) film was improved from $1.5x10^{-12}$ to 2.63 x 10^{-6} S/cm, more than 10 orders of magnitude below that measured for CNTs [11]. In a separate study, epoxy matrix composites made with aligned arc-discharge synthesized SWNTs yielded electrical conductivity improvements from $1x10^{-16}$ S/cm for epoxy to 1.2 x 10^{-5} S/cm at a 7.0 wt.% loading of aligned SWNTs. The tensile modulus in the direction of the aligned tubes exhibited an average increase of 165%, and tensile strength in the axial direction of the aligned tubes

increased by 300% relative to the epoxy matrix. However, in the direction 90° to the aligned SWNTs, the tensile strength was reduced by 25% below the measured strength of the pristine epoxy[12]. This study indicates the importance of tube alignment to mechanical performance. The poor performance in the orthogonal direction suggests that these CNT composites are highly anisotropic, with the CNT acting as a defect in the perpendicular loading direction. Some of the most promising results for structural CNT composites to-date are attributed to Wang, et.al [13] where acetone condensed sheets of MWNTs synthesized by Nanocomp Technologies, Inc. [14], were fabricated into bismaleimide (BMI) matrix composites. The CNTs were mechanically stretched by 40% to align the MWCNTs within the sheets. The resulting MWNT/BMI composites had an average of 60 ± 2 wt.% CNTs with a density of 1.525 g/cc. Assuming a density of 1.8 g/cc for the MWNTs and 1.25 g/cc for the BMI resin, this yields a fiber volume fraction (FVF), of 50.83%; an order of magnitude higher than previous work with dispersed tubes. For the composite fabricated from the 30% extension-ratio stretched sheet, the electrical conductivity parallel to the aligned MWNT was σ_1 = 1,800 S/cm and for those from the 40% extension-ratio stretched sheet, σ_1 = 5,500 S/cm. Mechanical testing of the MWNT/BMI composite containing the 40% extension-ratio stretched sheet resulted in a tensile failure strength as high as 2.1 GPa and a tensile modulus up to 169 GPa [13]. When normalized for FVF, these values exceed the reported tensile strength and modulus of uni-tape IM7/BMI CFRP. These initial results are part of the impetus for the ongoing effort at NASA LaRC to further investigate the Nanocomp MWNT sheets with various pretreatments and polymer matrices for potential application in future aerospace composite structure.

2.0 EXPERIMENTAL

2.1 Materials

The composite prepreg material utilized in this effort is the toughened-epoxy, intermediate modulus carbon fiber with 12,000 filaments per tow (12k) Hexcel IM7/8552 with 35% resin content and fiber areal weight (FAW) of 135 g/m^2. The cured ply thickness of this version of the Hexcel prepreg is reported to be 0.131 mm (0.0052 in) [7]. This material is a well-characterized aerospace CFRP. The b-basis design allowables are available in both CMH-17 and in the AGATE database.

The Hexcel 8552 toughened-epoxy could not be obtained in neat resin form for the purpose of pre-impregnating the CNT sheet material. Therefore, the toughened epoxy API-60 was supplied by Applied Poleramic, Inc., Benicia, CA, USA with properties similar to Hexcel 8552 (tensile strength of 121 MPa and an elastic modulus of 4.7 GPa). API-60 was used to pre-impregnate the CNT sheets as a 50 wt% solution of epoxy in methyl ethyl ketone (MEK).

The CNT sheet material was supplied by Nanocomp Technologies, Inc., Merrimack, NH. This material is supplied as batches corresponding to large sheets with dimensions up to 122 x 244 cm containing both single-wall and few-wall CNT. The typical FAW of the acetone treated Nanocomp sheets is 10 ± 3 g/m^2. An SEM image typical of as-received Nanocomp CNT sheets is provided in Figure 1. The tubes are approximately 1 mm in length with diameters ranging from 5 to 10 nm. The CNTs are synthesized by a chemical vapor deposition (CVD)-like proprietary process [14]. The CNT sheet batches, lot #4007 and lot #5768, used in this study were treated at Nanocomp with acetone to condense the sheets which are 25 ± 5 μm thick. The acetone densification is the only chemical pretreatment of the CNTs utilized in this study. The

supplied sheets possess an inherent directionality due to the drawing process utilized at Nanocomp. The direction in which the mats of CNTs are collected during the synthesis process is termed the 0° direction and result in supplier reported tensile failure strengths of 400 ± 50 MPa. Reported 90° average tensile strength is typically 20-30% lower than that measured parallel to the sheet take-up direction.

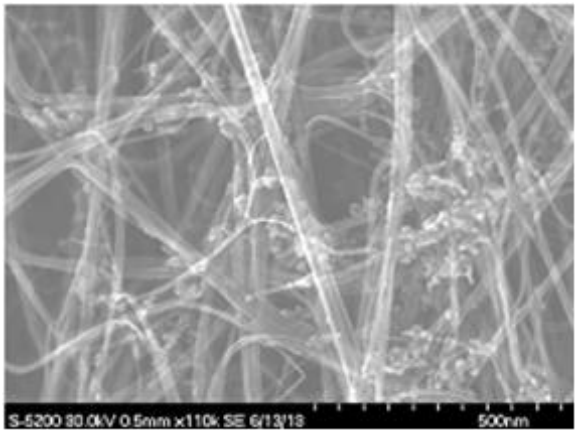

Figure 1. Image from High Resolution SEM of as-received CNT sheet surface, 1 x 1 μm area.

2.2 Hybrid CNT Composite Fabrication

The fabrication of the IM7/8552 hybrid laminates containing CNT sheets was dictated by the type of characterization to be performed. For example, in-plane thermal diffusivity characterization by laser flash analysis (LFA) required laminate specimens with nominal thickness < 0.5 mm (0.02 in). Mechanical characterization of the hybrid CNT composites required fabrication of laminates containing 20 plies of IM7/8552 prepreg for SBS testing and 32 plies for the fracture toughness testing. Electrical resistivity characterization was performed using specimens extracted from both the thin and thick laminates. The Nanocomp supplied CNT sheets were mechanically stretched in the 0° direction to ~121% of the original specimen length to improve the alignment of the CNTs following a LaRC developed procedure [15-16]. Due to necking of the deformed sheet during the stretching procedure, the resulting aligned CNT sheets were 7.6 x 7.6 cm, which dictated the dimensions of the hybrid laminate panels fabricated for the purpose of thermal, electrical and SBS characterization. To obtain double cantilever beam (DCB) and end notch flexure (ENF) coupons, panels having dimensions of 30.5 x 30.5 cm were fabricated by interleaving the 7.6 x 7.6 cm aligned, pre-infused CNT sheets adjacent to the 12.5 μm thick Teflon "crack-starter" film between the 16^{th} and 17^{th} plies of IM7/8552 in the configuration shown in Figure 2.

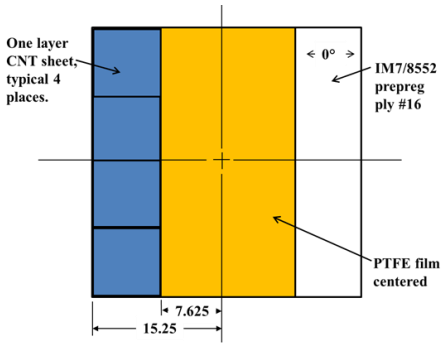

Figure 2. Lay-up configuration of Hybrid CFRP panels for DCB and ENF coupons.

The term "pre-infusion" refers to the process utilized to introduce polymer matrix to the CNT sheet prior to adding the material into the stack of uncured IM7/8552 prepreg. In this study, the pre-infusion process involved coating the CNT sheet using a measured quantity of solution of API-60 in MEK. Suspending the epoxy in a solution of MEK at 50% polymer solids resulted in a Brookfield viscosity of 0.2 Pa•sec, which facilitated hand-painting of the resin solution on the surface of the stretched sheets. Prior to application of the epoxy-MEK solution, each 7.6 x 7.6 cm CNT sheet, both stretched and un-stretched, was weighed to three significant figures using a calibrated analytical balance resulting in an average mass prior to infusion of 0.067 ±0.003 g. Therefore, all pre-infused CNT sheets were uniformly coated on one side with a quantity of 0.08 +/-0.004 g of API-60/MEK solution, as confirmed by weighing the sheets after application of the resin solution. While the mass of API-60 applied to each sheet was consistent and results in an average of 50% by wt. resin content, the uniformity of the application was not determined by any method other than visual observation, and therefore is unknown. After coating the sheet with the resin solution, the sheets were placed in a chemical hood at 25°C for 24 hours prior to being interleaved in the prepreg stack, during which an average of 30% by wt. of MEK evaporated from each sheet. All of the composite laminates fabricated in the current study, hybrids and controls, were placed in a stainless steel mold with the 0° direction of the CNT sheets aligned with the 0° direction of the carbon fibers and cured in a vacuum press following the Hexcel recommended IM7/8552 cure cycle. The fabricated control and hybrid CNT composite panels, stacking sequence, and CNT sheet pretreatment parameters studied in this effort are listed in Table 1., where the term "S" refers to stretched and "I" refers to pre-infused.

Table 1. Composite Panel Fabrication Details

Property Characterization	Panel dimensions (cm)	Panel Designation	CNT Sheet pretreatment	Number of IM7/8552 plies	Stack orientation
Thermal and Electrical Conductivity	2.54 x 2.54	Control-T	None	2	$[0]_2$
		T-A	None	2	[0/CNT/0]
		T-B	I	2	[0/CNT/0]
		T-C	S/I	2	[0/CNT/0]
SBS Strength and Electrical Conductivity	2.54 x 2.54	Control-SBS	None	20	$[0]_{20}$
		SBS-A	None	20	$[0/CNT]_{20}$
		SBS-B	I	20	$[0/CNT]_{20}$
		SBS-C	S/I	20	$[0/CNT]_{20}$
		SBS-D	S/I	20	$[0_{10}/CNT_5/0_{10}]$
Mode I Fracture Toughness	30.5 x 30.5	Control-DCB	None	32	$[0]_{32}$
		CNT-DCB	S/I	32	$[0_{18}/CNT/0_{18}]$
Mode II Fracture Toughness	30.5 x 30.5	Control-ENF	None	32	$[0]_{32}$
		CNT-ENF	S/I	32	$[0_{18}/CNT/0_{18}]$

2.3 Photo-microscopy of fabricated panels

One 2.54 x 1.27 cm specimen was obtained by cutting a specimen from the center of each of the five 7.6 x 7.6 cm panels fabricated using a wet-saw. The edge of each of these specimens was polished and analyzed under an optical microscope to determine the general consolidation quality of the composite laminate. Photomicrographs were obtained and are presented in Section 3.1.

2.4 Electrical Conductivity Characterization

One 2.54 x 2.54 cm specimen was obtained from each of the four 7.62 x 7.62 cm $[0]_{20}$ panels fabricated, including specimens from SBS-control panels and the three hybrid CNT panels. To remove any residual resin on the specimen surfaces, they were hand polished using 400-grit SiC paper. In-plane direct current (DC) conductivity measurements were carried out using the in-line method and the Montgomery method for anisotropic materials [17]. For the inline measurements, a Signatone probe station was used with the samples rotated under the probes. For the Montgomery method measurement, a custom test head was assembled with 4 gold plated, spring loaded pins (pogo pins) placed 2.54 cm apart on a printed circuit board. In both cases, a Keithley (KE) 2400 current source and KE 2000 digital multimeter were used.

2.5 Thermal Conductivity Characterization

The thermal conductivity property of a material is the quantity of (heat) energy which flows through a unit length, in unit time, when there is a unit temperature difference between the two ends of the length. The thermal conductivity of the control and hybrid CNT laminates was measured according to ASTM E1461 [18]. Thermal conductivity, λ, was calculated according to:

$$\lambda = \alpha(C_p \bullet \rho)$$

Where, ρ is the material density (g/cc), C_p is the specific heat capacity (J/K), and α is the thermal diffusivity (m^2/s) measured using the pulse method provided in laser flash analysis (LFA). A 2.54 cm diameter disk was obtained using a carbide hole-punch from a $[0]_2$ IM7/8552 panel and each of the thin laminate panels fabricated using one sheet of CNT sandwiched between two plies of IM7/8552, labelled T-A, T-B, and T-C in Table 1. The heat capacity of each of these laminates was determined at 25°C and 100°C using modulated differential scanning calorimetry on a Netzsch DSC 204 F1 Phoenix®. The through-thickness and in-plane thermal diffusivity was characterized at 25°C and 100°C using a Netzsch LFA-457 MicroFlash®.

2.6 Short Beam Shear Testing

The SBS strength was determined for each of the laminates containing 20-plies of IM7/8552 and interleaved CNT sheet following the testing standard for SBS, ASTM D2344 [19]. Since the average thickness of the control and three hybrid panels was 2.70 ± 0.25 mm, all of the coupons were cut using a wet-saw into 1.27 x 0.64 cm coupons. Due to the small thickness variation from panel to panel from the addition of CNT sheets, the support span was altered for each coupon set to maintain a thickness-to-span ratio of 4.0 according to the standard. In displacement control, the loading-nose traveled at a rate of 1 mm/min (0.05 in/min).

2.7 Fracture Toughness Testing

2.7.1 Mode I DCB Testing

Four $[0]_{32}$ IM7/8552 DCB coupons and six hybrid DCB coupons fabricated using $[0]_{32}$ IM7/8552 containing one layer of stretched and infused (S/I) CNT sheet located mid-plane in the prepreg stack as shown in Figure 3. The 15.24 x 2.54 cm control and hybrid coupons were all obtained from the one fabricated 30.5 x 30.5 cm panel. A 12.5 mm thick Teflon crack starter was located at the center of the laminate stack extending from one machined end of the coupon 7.62 cm into the coupon and across the coupon width according to recommendations in ASTM D5528 [20]. Prior to testing, 2.54 cm piano hinges were bonded to the top and bottom plies of the DCB coupons following methods described in [21]. All ten DCB coupons, including four control and six hybrid CNT laminates, were tested at room temperature using an MTS-858 table-top servo-hydraulic test frame with a calibrated 2250 N load cell. After statically pre-cracking each coupon, the piano hinges were loaded in tension under displacement control at a rate of 1.27 mm/min until the crack propagated 40 mm. For both the pristine IM7/8552 $[0]_{32}$ laminate as well as the hybrid CNT $[0_{16}/(\text{CNT-SI})_1/0_{16}]$ laminate, the fracture toughness, G_{IC}, was calculated using the Modified Beam Theory (MBT):

$$G_{IC} = \frac{3P\delta}{2b(a+\Delta)}$$

Where, the crack extension or delamination length, *a* (mm), was recorded at approximately every millimeter of stable crack growth in addition to the corresponding applied load, *P* (N), and the load-point displacement, δ (mm). The term Δ is the delamination length correction factor determined by a least squares linear fit of the observed delamination lengths, *a*, versus the cube root of the corresponding compliance [20-21].

After DCB testing of ten coupons, the pristine fracture surface approximately 15 mm from the crack initiation of one coupon from each material set was inspected by photo-microscopy at 50X and 500X. The same surfaces were imaged using a Hitachi Model S-5200 field emission-scanning electron microscope (FE-SEM) equipped with an in-lens detector. The FE-SEM samples were prepared by extracting an approximately 2 mm × 3 mm size specimen from the same fracture surface region of each of the DCB coupons analyzed in photo-microscopy and exposed to the electron beam without additional coating on the sample surface. SEM images were taken at 15 keV of accelerating voltage and 20 μA of beam current.

2.6.2 Mode II ENF Testing

The Mode II interlaminar shear fracture toughness of the hybrid laminate was determined using the End Notch Flexure (ENF) test method described in [22-23]. This testing methodology is currently under revision by ASTM as a possible standard test method. The ENF test involves loading a 17.8 cm long x 2.54 cm wide composite beam in three point bending. The laminate coupon contains a 7.62 cm long 12.5 μm thick Teflon insert at the mid-plane of the $[0]_{32}$ laminate coupon to facilitate the crack initiation. In this study, ENF testing was conducted on both control coupons and hybrid CNT laminate coupons extracted from one cured 30.5 cm x 30.5 cm panel laid-up according to Figure 2. The stretched and infused CNT sheets were placed adjacent to the Teflon insert between plies 16 and 17 of the $[0]_{32}$ IM7/8552 stack prior to cure in a vacuum press. After statically pre-cracking each coupon in the 3-point bend fixture, a least-squares linear regression of the resulting load vs stroke data was utilized to calculate the compliance calibration (CC) coefficient, m, as described in [26]. The PC coupon was repositioned and subsequently loaded to advance the delamination with the force, *P* (N), loading roller displacement δ (mm), and crack delamination length, *a* (mm), recorded. The Mode II fracture toughness of the pre-crack coupon was then calculated using the coupon width of B = 25.4 mm and the following:

$$G_{IIC} = \frac{3mP_{\max}^2 a_0^2}{2B}$$

The compliance calibration curves as well as the PC G_{IIC} resulting from ENF testing are reported for the $[0]_{32}$ IM7/8552 laminate and the hybrid laminate containing one layer of S/I CNT sheet in the Section 3.5.

3.0 RESULTS AND DISCUSSION

3.1 Photo-Microscopy

The consolidation quality of the 7.6 x7.6 cm $[0]_{20}$ IM7/8552 (Control) and the four hybrid panels were determined by optical microscopy. Figures 3 and 4 show the photo-microscopy images of these panels taken at 50X and 200X magnification, respectively. In these images the IM7 carbon fibers and the CNT run parallel to the surface of the image.

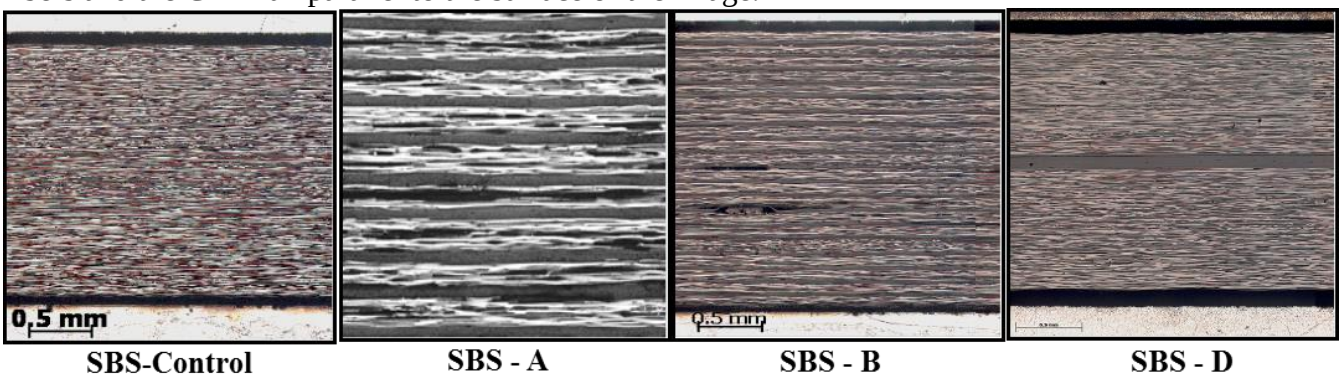

Figure 3. Photo microscopy at 50X of the control and three hybrid CNT composite panels

As shown in the photo-microscopy in Figures 3 and 4, the $[0]_{20}$ IM7/8552 SBS-Control laminate is well-consolidated with low porosity. There is a significant difference in the quality of the SBS-C laminate versus the SBS-A, each of which contain a layer of CNT sheet between each ply of IM7/8552. The high porosity evident in the IM7/8552 plies in the SBS-A panel fabricated using 19 sheets of the pristine (un-infused) CNT sheet is likely due to flow of the 8552 epoxy resin out of the prepreg and into the dry/pristine CNT sheets during the elevated temperature cure cycle when the epoxy resin reaches its minimum viscosity prior to gelation, or cure. Photo-microscopy of the SBS-Control and the two hybrid CNT composites containing stretched and infused sheets of CNT are also shown below in Figure 4.

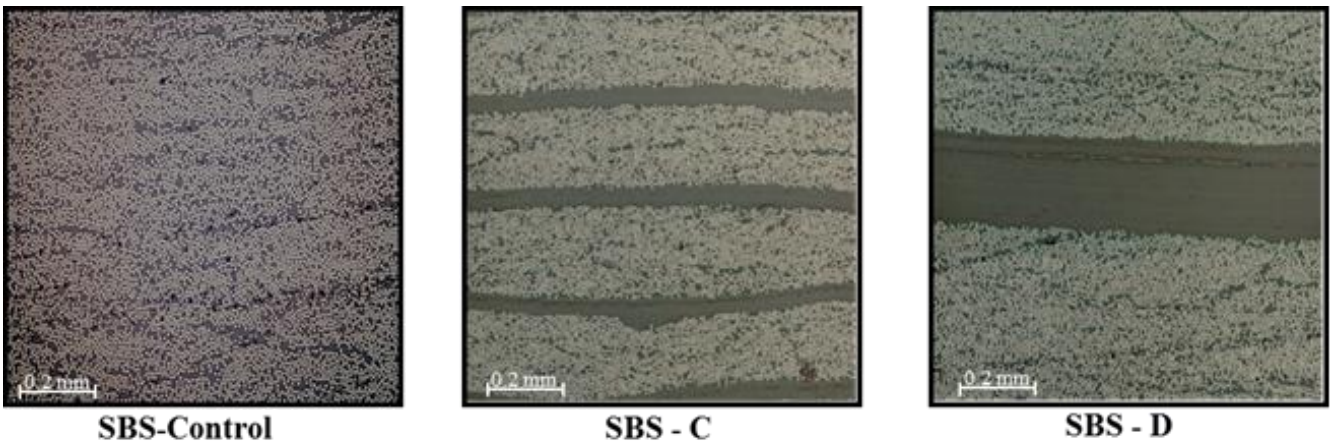

Figure 4. Photo-microscopy of control and the stretched/pre-infused hybrid CNT composite at 200X

These micrographs were taken of the surface of the laminate orthogonal to the direction of the carbon fibers and the aligned tubes. At this level of magnification only minimal micro-voids are observed in the laminate and the carbon fiber are uniformly distributed in the epoxy matrix;

indicative of CFRP with FVF ≈60% and void volume fraction (VVF) ≤2%. At this magnification, no conclusions can be made regarding the FVF or VVF of the CNT layers. Again, it is clear that the pre-infusion of the CNT sheets, improves the quality of the hybrid laminates

3.2 Electrical Conductivity of Hybrid CNT Composites

The in-plane electrical resistivity was determined for the 2.54 x 2.54 cm specimens in both the 0° and 90° directions. To confirm the trends observed, specimens were characterized from both the control and hybrid thin $[0]_2$ thermal conductivity panels and the thicker $[0]_{20}$ laminates prepared for SBS testing. The hybrid panels contained CNT sheets with different pretreatments, including pristine (as-received), pre-infused (I) and stretched and infused (S/I). The in-plane electrical resistivity, ρ, of the uni-directional laminates was measured and the results were used to calculate the electrical conductivity, $\sigma = 1/\rho$, in units of Siemens/cm (S/cm) reported in Table 2. For the thicker laminates, in both laminate directions the electrical conductivity increases with increased volume of CNT material except for the SBS-A panel, containing the pristine CNT sheets.

Table 2. In-Plane 0° and 90° electrical resistivity measurement results of IM7/8552 and Hybrid laminates.

Panel Designation	CNT Sheet pretreatment	Stack orientation	In-plane 0° Resistivity (Ω cm)	In-plane 90° Resistivity (Ω cm)	In-plane 0° Conductivity (S/cm)
Control-T	None	$[0]_2$	0.05	0.17	19.90
T-A	None	[0/CNT/0]	0.01	0.06	143.27
T-B	I	[0/CNT/0]	0.00	0.06	403.23
T-C	S/I	[0/CNT/0]	0.00	0.06	436.68
Control-SBS	None	$[0]_{20}$	0.59	2.14	1.70
SBS-A	None	$[0/CNT]_{20}$	0.82	3.43	1.21
SBS-C	S/I	$[0/CNT]_{20}$	0.02	0.70	48.90
SBS-D	S/I	$[0_{10}/CNT_5/0_{10}]$	0.50	1.88	1.98

The consistently poor performance of the SBS-A laminate is due to the high porosity shown in Figure 3. The conductivity results for this laminate as well as the mechanical performance discussed in Section 3.4 confirm that the CNT sheets must be infused with polymer matrix prior to interleaving into the CFRP prepreg stack. In both the thick and thin laminates, the results indicate that the increase in the in-plane electrical conductivity parallel to the direction of the carbon fiber and the aligned (S/I) CNTs is significantly higher than the unaltered IM7/8552 laminate.

3.3 Thermal Conductivity of Hybrid CNT Composites

The thermal conductivity of the hybrid CNT composites was characterized by laser flash analysis. The results of through-thickness and in-plane thermal conductivity characterization are provided in Table 3. This characterization was conducted using specimens containing two unidirectional plies of IM7/8552 $[0]_2$ (control). The thermal conductivity is also reported for hybrid composite specimens containing a single CNT sheet with various pre-treatments sandwiched between two plies of IM7/8552.

Table 3. Thermal conductivity of IM7/8552 and hybrid CNT composites.

Panel Designation	CNT Sheet Pretreatment	Stack Orientation	Heat Capacity (J/g)		Through Thickness Thermal Conductivity (W/m*K)		In-plane Thermal Conductivity (W/m*K)	
			25°C	100°C	25°C	100°C	25°C	100°C
Control-T	None	$[0]_2$	0.938	1.165	1.022	1.145	5.495	6.094
T-A	None	[0/CNT/0]	0.917	1.150	1.193	1.176	5.335	5.807
T-B	I	[0/CNT/0]	0.845	1.076	1.227	1.388	5.368	6.224
T-C	S/I	[0/CNT/0]	1.042	1.279	1.269	1.448	6.223	6.702

As expected, the through-thickness thermal conductivity is lower than the in-plane thermal conductivity, which increases with temperature in both of the laminate directions. However, based on these results, the interleaving of the CNT sheets does not have a significant impact on the in-plane thermal conductivity of the CFRP laminate. The alignment of the nanotubes by stretching the sheets was found to have a minor positive influence on the measured in-plane thermal conductivity. It is also possible that the LFA method is not the proper approach for characterizing the in-plane thermal conductivity of an orthotropic material and that the "guarded hot-plate" characterization methodology may be a more appropriate technique to measure the effects of the CNT sheets on the thermal conductivity of a structural CFRP laminate.

3.4 Short Beam Shear Strength of Hybrid CNT Composites

The SBS strength was determined according to ASTM D2344. The coupons were extracted from the same four 7.6 x 7.6 cm 20-ply IM7/8552 control and hybrid panels used to conduct electrical conductivity characterization. The average and coefficient of variation (CoV) values reported in Table 4 are based on six valid SBS failures for each panel type according to the ASTM standard description of edge failure. The room temperature dry (RTD) SBS strength of an IM7/8552 0° laminate is reported by Hexcel as 137.2 MPa which agrees well with the average of 132 .2 ±1.51 MPa found for the control coupons tested using the $[0]_{20}$ IM7/8552 laminate.

Table 4. SBS strength of IM7/8552 control and three hybrid CNT composites.

Panel Designation	CNT Sheet Pretreatment	Stack Orientation	Average Coupon Thickness (mm)	SBS Strength (Mpa)	CoV (%)
Control-SBS	None	$[0]_{20}$	2.49	132	1.14
SBS-A	None	$[0/CNT]_{20}$	2.55	44	4.48
SBS-B	I	$[0/CNT]_{20}$	2.96	101	1.90
SBS-C	S/I	$[0/CNT]_{20}$	2.87	98	2.05
SBS-D	S/I	$[0_{10}/CNT_5/0_{10}]$	2.50	122	3.06

The lowest average SBS failure strength was found for the hybrid containing pristine sheets of CNT. This low strength is attributed to the poor consolidation and high porosity found in this laminate (Figure 3) due to bleed-out of the 8552 epoxy from the IM7/8552 prepreg into the CNT layers. The higher strength for SBS-B containing 19 pre-infused CNT sheets reinforces the importance of this pre-treatment. Stretching of the CNT sheet to align the tubes does not result in significant improvement of the SBS strength in the laminate containing a quantity of 19- CNT

sheets interleaved uniformly throughout the thickness of the $[0]_{20}$ IM7/8552 laminate. The high SBS strength found for the SBS-D hybrid panel may indicate that the location of the CNT sheet in the CFRP can be further optimized or that the CNT sheet resin content in the other hybrid panels is not optimized. Additionally, while the CNT alignment has been demonstrated to improve the tensile properties of CNT composites in other studies, this pre-treatment may not impact the inter-laminar properties of the hybrid laminates. The inter-laminar and shear properties of the laminate are more likely to be affected by the CNT interaction with the polymer matrix.

3.5 Mode I and Mode II Fracture Toughness of Hybrid CNT Composites

To determine why the SBS strength is reduced with the introduction of the infused CNT layers, the Mode I and Mode II fracture toughness at the location of the CNT sheet interface was measured by the DCB and ENF test methods, respectively. From the DCB testing, force-displacement curves typical of the pre-cracked (PC) tests from both the four $[0]_{32}$ IM7/8552 control coupons and the six hybrid laminate coupons are shown in Figure 5. The average G_{IC} values obtained from DCB testing are summarized with the ENF results in Table 5. Fractography conducted using SEM of the DCB failure surfaces for the IM7/8552 control laminate in the pre-crack region ≈ 13 mm from the Teflon insert crack-starter are shown in Figure 6.

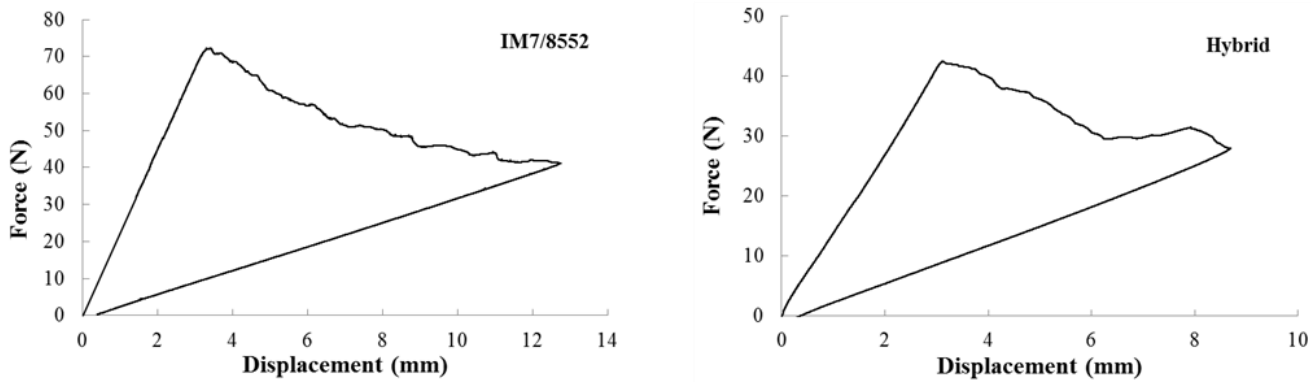

Figure 5. Typical force-displacement curves for IM7/8552 (Control) and Hybrid CNT composite DCB coupons.

Table 5. Mode I and Mode II fracture Toughness Results

Panel Designation	CNT Sheet Pretreatment	Stack Orientation	Number Test Coupons	G_{IC} (J/m^2)	Standard Deviation (J/m^2)	G_{IIC} (J/m^2)	Standard Deviation (J/m^2)
Control-DCB	None	$[0]_{32}$	4	239.90	7.18	N/A	N/A
CNT-DCB	S/I	$[0_{16}/CNT/0_{16}]$	6	117.32	12.26	N/A	N/A
Control-ENF	None	$[0]_{32}$	4	N/A	N/A	677.68	71.8
CNT-ENF	S/I	$[0_{186}/CNT/0_{16}]$	6	N/A	N/A	1358.85	182.11

The diagnostics of the resulting image are consistent with Mode I fracture of toughened epoxy CFRP, including textured micro-flow in the resin regions adjacent to the carbon fiber tracks.

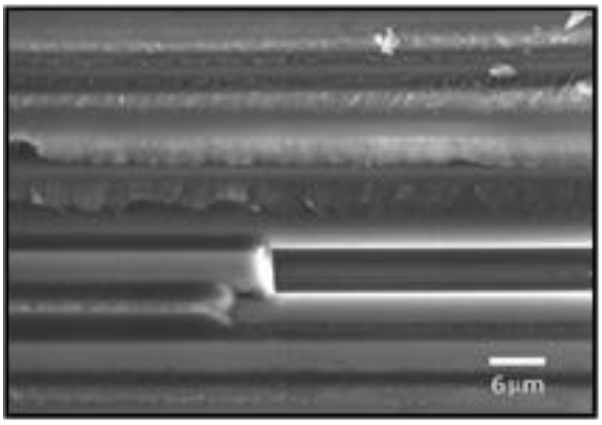

Figure 6. HR-SEM image of the PC region of the DCB failure surface of the IM7/8552 control laminate.

Fractography of the DCB failure surfaces of the hybrid laminate containing the stretched/infused layer of CNT sheet adjacent to the Teflon crack-starter was conducted by imaging the surfaces at approximately the same distance along the pre-cracked coupon. These images are shown in Figure 7.

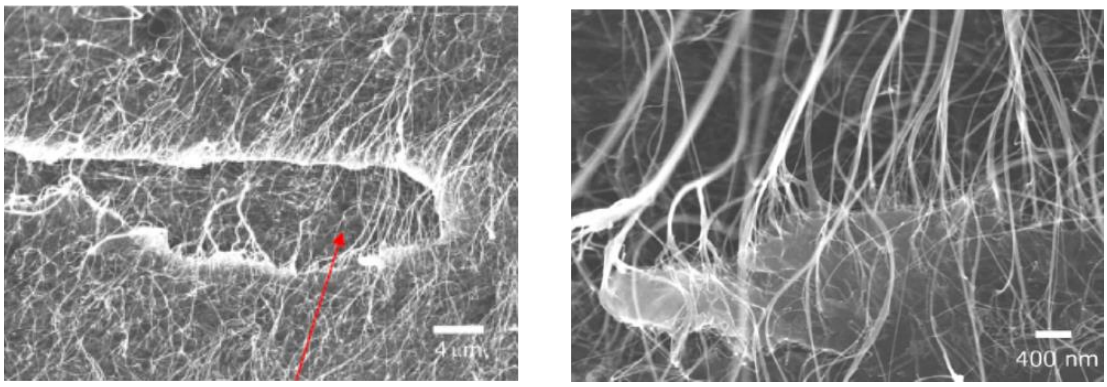

Figure 7. SEM images of PC region of the DCB failure surface of the hybrid CNT laminate.

Macroscopic and microscopic fractography of the DCB PC failure surfaces of the hybrid laminates revealed no carbon fibers; indicating that the crack traversed through the ≈25μm thick S/I CNT sheet layer. The DCB results provide insight into the fracture toughness of the intralaminar CNT sheet rather than the interlaminar toughness between the IM7/8552 laminate ply and the CNT sheet. The arrow in the left image of Figure 7 points to the fracture region that is then imaged at subsequently higher magnification on the right. In the higher magnification image, individual CNTs appear to be pulled away, or "released", from a region of deformed polymer resin. At this magnification, the "released" CNTs do not appear to have any polymer adhered to the surfaces. There is also no evidence that any of the CNTs are fractured.

The average Mode II fracture toughness was investigated by ENF testing of four $[0]_{32}$ IM7/8552 laminate coupons and six hybrid CNT laminate coupons obtained from one 30.5 x 30.5 cm panel. The PC compliance calibration coefficient, m, of the laminate coupons was determined by linear

regression according to the method described in [22-23] the resulting fit of the data are shown in Figure 8 for both the control and the hybrid CNT laminates.

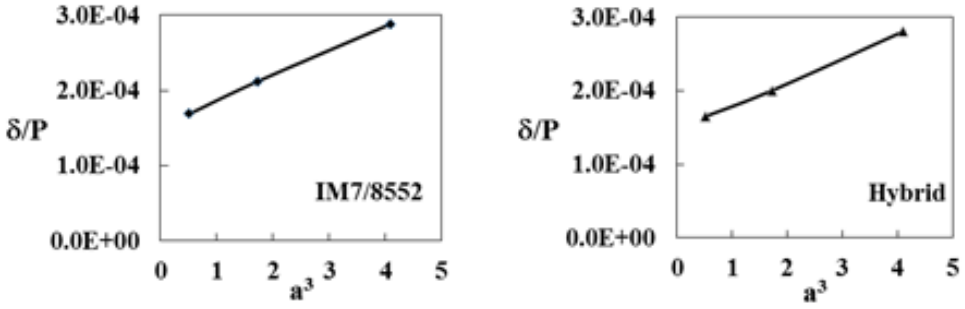

Figure 8. Typical fit of compliance as a function of crack length for NPC fracture test for the IM7/8552 (Control) and the Hybrid CNT laminates.

The average value of the Mode I Fracture Toughness, G_{IC}, found for the IM7/8552 DCB control coupons in this study is comparable to the value of 0.221 kJ/m^2 (1.37 in-lb/in^2) calculated by the MBT method reported by Czabaj [21] for $[0]_{32}$ IM7/8552. The average interlaminar shear fracture toughness, G_{IIC}, found for the IM7/8552 ENF control coupon closely matches the value of average G_{IIC} = 738.96 J/m^2 (4.22 in-lb/in^2) reported by O'Brien [22] calculated using the compliance calibration data reduction method of ENF data for IM7/8552.

The significant reduction of the Mode I fracture toughness for the hybrid CNT laminate is likely due to poor CNT adhesion to the polymer matrix, which is supported by the fractography images in Figure 7. The increase in the Mode II fracture toughness for the hybrid CNT laminate is contrary to the results expected based on the reduced SBS strength of the pre-infused hybrid composite. These results are similar to previous results published by Nguyen [24] for hybrid CNT laminates fabricated using different CNT sheet material and processing techniques. Future work involving fractography of the ENF coupons is planned, and anticipated to provide additional insight into the observed results.

4.0 Summary

The 0° in-plane electrical conductivity of the aerospace CFRP IM7/8552 was significantly increased by interleaved layers of aligned and pre-infused layers of Nanocomp CNT sheets. LFA characterization indicates that for the same volume loading and pretreatment of the CNT, the thermal conductivity of the laminate is not significantly increased. SBS testing of the hybrid laminate indicates that the resin content of the CNT sheet has the most significant influence on this interlaminar property. The DCB testing of the hybrid laminate resulted in intralaminar failure in the CNT layer. This G_{IC} value was half of that found for the CFRP control laminate, likely due to poor CNT adhesion to the polymer matrix. ENF testing of the hybrid laminate resulted in a doubling of the G_{IIC} value in comparison to the CFRP control laminate

5.0 ACKNOWLEDGEMENTS

The authors thank William Johnston of Science and Technology Corporation in residence at NASA LaRC, for his assistance in the DCB and ENF testing and data reduction.

6.0 REFERENCES

1. Reid, Chris; "Aviation Outlook: Fuel Pricing Ignites Demand for Composites in Commercial Transports", High Performance Composites, July, 2008.
2. Ogasawara, T., Hirano, Y., and A. Yoshimura; "Coupled Thermal Electrical Analysis for Carbon Fiber/Epoxy Composites Exposed to Simulated Lightning Current", *Composites: Part A*, Vol. 41, pp973-981, 2010.
3. Iijima, S., "Helical Microtubules of Graphitic Carbon", *Nature*, Vol. 354, pp56-58, 1991.
4. Salvetat-Delmotte, J.P. and A. Rubio; "Mechanical Properties of Carbon Nanotubes: A Fiber Digest for Beginners", *Carbon*, Vol. 40, pp1729-1734, 2002.
5. Treacy, M.M.J., Ebeson T.W., Gibson, T.M.; "Exceptionally High Young's Modulus Observed for Individual Carbon Nanotubes", *Nature*, Vol. 381, pp680-687, 1996.
6. Walters, D.A., Ericson, L.M., Casavant, M.J., Liu, D.T., Smith, K.A., and R.E. Smalley; "Elastic Strain of Freely Suspended Single-Wall Carbon Nanotube Ropes", *Applied Physics Letters*, Vol. 47, No. 25, pp. 3803-3805, 1999.
7. Hexcel Corporation, HexTow IM7 Carbon Fiber: Product Data, http://www.hexcel.com/resources/datasheets/carbon-fiber-data-sheets/im7.pdf.
8. Zhou, C., Kong, J., and H. Dai; "Intrinsic Electrical Properties of Individual Single-Walled Carbon Nanotubes with Small Band Gaps", *Physical Review Letters*, Vol. 84, No. 24, pp. 5604-5607, 2000.
9. Pop, E., Mann, D., Wang, Q., Goodson, K., and H. Dai; "Thermal Conductance of an Individual Single-Wall Nanotube above Room Temperature", *Nano Letters*, Vol. 6, No. 1, 2006.
10. Lee, R.S., Kim, H.J., Fischer, J.E., Thess, A and R.E. Smalley; "Conductivity Enhancement in Single-Walled Nanotube Bundles doped with K and Br", *Nature*, Vol. 388, No. 17, pp.255-256, 1997.
11. Anand, A.K., Agarwal, U.S., Nisal, Anuya, Joseph, Rani; "PET-SWNT Nanocomposites through Ultrasound Assisted Dissolution-Evaporation", *European Polymer Journal*, Vol. 43, pp.2279-2285, 2007.
12. Wang, Q., Dai, J., Li, W., Wei, Z., and J. Jiang; "The Effects of CNT Alignment on Electrical Conductivity and Mechanical Properties of SWNT/Epoxy Nanocomposites", *Composites Science and Technology*, Vol. 68, pp.1644-1648, 2008.
13. Cheng, Q., Bao, J., Park, J., Liang, Z., Zhang, C., and B. Wang; "High Mechanical Performance Composite Conductor: Multi-Walled Carbon Nanotube Sheet/Bismaleimide Nanocomposites", *Journal of Advanced Functional Materials*, Vol. 19, pp.3219-3225, 2009.
14. Lashmore, D.S., Braden, R., Anastasios, J.H., Welch, J., et.al; "Chemically-Assisted Alignment Of Nanotubes Within Extensible Structures", U.S. Patent 8246886 B2, August 21, 2012.
15. Hull, Brandon Tristan, "Development and Implementation of Tensile Testing Methodologies for the Examination of the Effects of Carbon Nanotube Sheet Stretching on Nanotube Alignment and Corresponding Mechanical Property Enhancement", Master's Thesis, Virginia Polytechnic and State University, 2013.
16. Cano, R.J., Grimsley, B.W., Czabaj, M.W., Hull, B.T., and E.J. Siochi; "Processing and Characterization of Carbon Nanotube Composites",SAMPE International Symposium,

Seattle WA, 2013.
17. Montgomery, H.C.; “Method for Measuring Electrical Resistivity of Anisotropic Materials”, Journal of Applied Physics, Vol. 42, 1971.
18. ASTM E1461; “Standard Test Method for the Thermal Diffusivity by the Flash Method”, ASTM International, 100 Barr Harbor Dr., West Conshohocken, PA, 2013.
19. ASTM D2344; “Standard Test Method for Short Beam Strength of Polymer Matrix Composites and their Laminates”, ASTM International, 100 Barr Harbor Dr., West Conshohocken, PA, 2006.
20. ASTM D5528; “Standard Test Method for Mode I Interlaminar Fracture Toughness of Unidirectional Fiber Reinforced Polymer Matrix Composites”, ASTM International, 100 Barr Harbor Dr., West Conshohocken, PA, 2007.
21. Czabaj, M.W., Ratcliffe, J.R., “Comparison of Intralaminar and Interlaminar Mode I Fracture Toughnesses of a Unidirectional IM7/8552 Carbon/Epoxy Composite”, *Composite Science and Technology*, Vol. 89, pp.15-23, 2013.
22. O’Brien, T.K., Johnston, W.M., and G.J. Toland; “Mode II Interlaminar Fracture Toughness of and Fatigue Characterization of a Graphite Epoxy Composite Material”, NASA Technical Memorandum, 216838, 2010.
23. Davidson, B., Ratcliffe, J.; “Draft Standard Test Method for Determination of the Mode II Interlaminar Fracture Toughness of Unidirectional Fiber Reinforced Polymer Matrix Composites Using the End Notch Flexure Test”, ASTM, 2011.
24. Nguyen, F.N., Tun, S., Haro, A.P., Hirano, N., Yoshioka, K., and R. Ovalle-Robles; “Hybridization of Interlaminar Reinforcements in Carbon Fiber Reinforced Polymer Composite”, SAMPE Technical Conference, Wichita, KS, 2013.